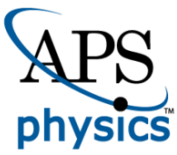

Emergence of Hilbert Space Fragmentation in Ising Models with a Weak Transverse Field

Atsuki Yoshinaga, Hideaki Hakoshima, Takashi Imoto, Yuichiro Matsuzaki, and Ryusuke Hamazaki

Phys. Rev. Lett. **129**, 090602 — Published 26 August 2022

DOI: 10.1103/PhysRevLett.129.090602

Emergence of Hilbert Space Fragmentation in Ising Models with a Weak Transverse Field

Atsuki Yoshinaga,[1,2,*] Hideaki Hakoshima,[2,3] Takashi Imoto,[2] Yuichiro Matsuzaki,[2,†] and Ryusuke Hamazaki[4,‡]

[1]*Department of Physics, The University of Tokyo, 5-1-5 Kashiwanoha, Kashiwa, Chiba 277-8574, Japan*
[2]*Research Center for Emerging Computing Technologies, National institute of Advanced Industrial Science and Technology (AIST), Central2, 1-1-1 Umezono, Tsukuba, Ibaraki 305-8568, Japan*
[3]*Center for Quantum Information and Quantum Biology, Osaka University, 1-2 Machikaneyama, Toyonaka 560-0043, Japan*
[4]*Nonequilibrium Quantum Statistical Mechanics RIKEN Hakubi Research Team, RIKEN Cluster for Pioneering Research (CPR), RIKEN iTHEMS, Wako, Saitama 351-0198, Japan*

The transverse-field Ising model is one of the fundamental models in quantum many-body systems, yet a full understanding of its dynamics remains elusive in higher than one dimension. Here, we show for the first time the breakdown of ergodicity in d-dimensional Ising models with a weak transverse field in a prethermal regime. We demonstrate that novel Hilbert-space fragmentation occurs in the effective non-integrable model with $d \geq 2$ as a consequence of only one emergent global conservation law of the domain wall number. Our results indicate nontrivial initial-state dependence for non-equilibrium dynamics of the Ising models in a weak transverse field.

Introduction. — The transverse-field Ising model (TFIM) serves as a minimal model among quantum many-body systems [1, 2]. Despite its simplicity, the TFIM is quite difficult to investigate in higher-than-one dimensions because of its non-integrable nature. It is particularly important for foundation of quantum statistical mechanics to elucidate dynamical properties of the model. Indeed, its quantum thermalization has recently been investigated in relatively large systems [3–7]. For example, ergodicity in the ordered phase is controversial in the two-dimensional TFIM [3, 4, 8]. It was found that the model does not always thermalize in some quenches with numerical experiments [8] and that non-thermal eigenstates exist in a two-dimensional ladder system in the weak transverse-field limit [9].

The search for understanding quantum thermalization and the conditions behind it has been expanded substantially [10–22] in the recent decades because of the progress in experimental techniques [23–30]. One of the most important achievements is the eigenstate thermalization hypothesis (ETH) [10–12, 15, 31], which conjectures that all energy eigenstates are thermal and provides a sufficient condition for thermalization in isolated quantum systems. While the ETH has been confirmed numerically in various systems [15, 32–38], there is also growing interest in models violating the ETH. The emergence of non-thermal eigenstates has often been attributed to extensively many local conserved quantities due to, e.g., integrability [21, 39–42] and localization [43–47]. The Hilbert space fragmentation (HSF, or shattering) has recently attracted much attention as yet another mechanism of invalidating the ETH in non-integrable models [48–62]. In some models such as fractonic systems [63, 64], kinetic constraints impose restrictions on the dynamics [49–51] and create frozen regions which dynamically divide the systems. This generates a fragmented structure of the Hilbert space with exponentially many nontrivial subspaces. In these cases, initial states cannot access the entire Hilbert space and fail to thermalize. For many previous models showing the HSF, the presence of at least two conserved quantities and the locality of the interaction were the origin of relevant kinetic constraints.

In this Letter, we show the emergence of non-ergodicity in a prethermal regime for Ising models with a weak transverse field on a hypercubic lattice in dimensions higher than one. In particular, by analytical calculations, we reveal for the first time that the effective model for the TFIM in the weak-transverse-field limit exhibits the HSF for $d \geq 2$. Notably, this effective model has only one global conserved quantity namely, the domain-wall (DW) conservation. The locality of the Hamiltonian and the DW conservation law leads to a kinetic constraint in the model (Fig. 1 (a)), and to the appearance of frozen regions. Due to the frozen regions, the Hilbert space is separated into exponentially many subspaces (Fig. 1 (b)). Consequently, the ETH breaks down and the effective model shows non-thermalizing behavior depending on the initial state. The emergence of frozen regions in our model is distinct from the ones in the previously studied models which require several conserved charges for exhibiting such frozen regions [49–51, 57]. For $d = 2$, we further demonstrate that rich dynamical properties are found in subspaces inside the DW sectors, including those found in non-integrable, integrable, and quantum many-body scarred systems [55, 65–67].

Model. — We consider the TFIM on a d-dimensional hypercubic lattice

$$\hat{H} = \hat{H}_{\mathrm{DW}} + h_x \sum_i \hat{\sigma}_i^x, \text{ with } \hat{H}_{\mathrm{DW}} := -\sum_{\langle i,j \rangle} \hat{\sigma}_i^z \hat{\sigma}_j^z, \quad (1)$$

where $\hat{\sigma}_i^\mu$ ($\mu = x, y, z$) denotes the Pauli spin operators at site i, $\langle i, j \rangle$ indicates that the sites i and j are neighboring, and h_x denotes the strength of the transverse field. While the DW number, i.e., the eigenvalues n_{DW} of $\sum_{\langle i,j \rangle}(1 - \hat{\sigma}_i^z \hat{\sigma}_j^z)/2$, is not conserved under the time evolution by $\hat{H}$ for finite h_x, it is approximately conserved for a long time if h_x is sufficiently small [68]. Indeed, from a first-order perturbation theory, we obtain the following effective Hamiltonian [9, 69]:

$$\hat{H}_{\mathrm{eff}} := \hat{H}_{\mathrm{DW}} + h_x \hat{H}_1, \text{ with } \hat{H}_1 := \sum_i \hat{\sigma}_i^x \hat{Q}_i, \quad (2)$$

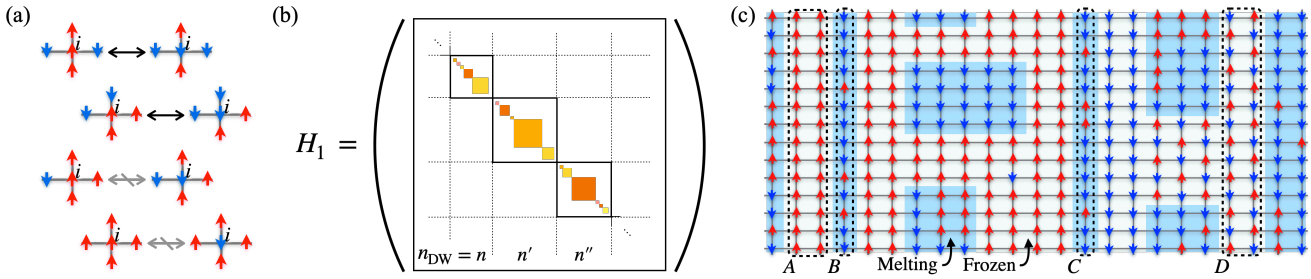

FIG. 1. (a) Schematic picture of the kinetic constraint arising from the projection operator $\hat{Q}_i$ in the Hamiltonian (2) where we take the dimension d as two. Each spin at site i on a square lattice is flipped only when its two nearest neighbors are up and the other two spins are down. (b) Fragmented structure of the effective Hamiltonian. In addition to the block structure due to the conservation of the domain-wall number $n_{\rm DW}$, the Hamiltonian matrix for an appropriate basis is further block diagonalized, namely fragmented. (c) An example of frozen regions (non-shaded) and melting regions (blue-shaded), where $d = 2$ and the periodic boundary condition is assumed. Red and blue arrows on each lattice site represent up and down spins in $\hat{\sigma}^z_i$ basis, respectively. The areas surrounded by dashed lines and labelled *A* and *D* exemplify prototypical spin configurations in frozen regions and those labelled *B* and *C* indicate one-dimensional melting regions which correspond to the PXP and XX models, respectively. Frozen regions percolate the system so that every spin in these regions is guaranteed to have at least three nearest-neighboring spins with the same sign.

where the operator $\hat{Q}_i$ projects all spin configurations onto the state space in which the sum of the z components of the $2 \times d$ spins surrounding the site i is zero (see Fig. 1 (a)). For example, the projector $\hat{Q}_i$ for $d = 2$ is explicitly given by [70]

$$\hat{Q}_i := \frac{5}{8} - \frac{1}{16}\left(\sum_{j\in \mathrm{ngbh}(i)} \hat{\sigma}^z_j\right)^2 + \frac{3}{8}\prod_{j\in \mathrm{ngbh}(i)} \hat{\sigma}^z_j, \qquad (3)$$

where $\mathrm{ngbh}(i)$ denotes the nearest-neighbor sites of the site i. The effective Hamiltonian $\hat{H}_{\rm eff}$ approximates the dynamics of local observables governed by the original Hamiltonian (1) for a certain time scale that goes to infinity as $h_x \to 0$ [70–72].

Since $\hat{H}_1$ commutes with $\hat{H}_{\rm DW}$, Hamiltonians $\hat{H}_1$ and $\hat{H}_{\rm eff}$ lead to the same dynamics when we specify a DW sector. Thus, we focus on the Hamiltonian $\hat{H}_1$ in the following. The Hamiltonian $\hat{H}_1$ is non-integrable as discussed later; it conserves the DW number and is block-diagonalized accordingly. Apart from spatial symmetries, such as inversion, the Hamiltonian also has global chiral symmetry, i.e., $\hat{H}_1$ anti-commutes with $\prod_i \hat{\sigma}^\nu_i$ $(\nu = y, z)$ [73]. This symmetry produces non-zero energy eigenvalues in pairs with opposite signs. While the Hamiltonian also has global $\mathbb{Z}_2$ symmetry (i.e., $\hat{H}_1$ commutes with $\prod_i \hat{\sigma}^x_i$), we confirm that this symmetry is irrelevant for the emergence of HSF.

Hilbert space fragmentation. — We now demonstrate the Hilbert-space fragmentation of $\hat{H}_1$ in each sector characterized by the number of DWs (see Fig. 1 (b)). We first show that the kinetic constraint induced by $\hat{Q}_i$ forms regions where the spin dynamics is frozen. More specifically, let us consider a product state $|F\rangle = \prod_{i\in\mathcal{F}} |s_i\rangle$ forming a sub-region $\mathcal{F}$ on the entire lattice Λ, where $|s_i\rangle$ is one of the eigenstates of $\hat{\sigma}^z_i$. If $|F\rangle$ satisfies the following condition, we call $\mathcal{F}$ a frozen region: $\hat{Q}_i(|F\rangle \otimes |M\rangle) = 0$ for $\forall i \in \mathcal{F}$ and any $|M\rangle$ defined on $\Lambda/\mathcal{F}$. The frozen regions remain unchanged under the time evolution by $\hat{H}_1$ (as well as $\hat{H}_{\rm eff}$). Meanwhile, non-frozen regions, which we call melting regions, are isolated from one another separated by frozen regions. Nontrivial dynamics occurs only in the melting regions. Below we focus on the case with $d = 2$ although most observations here hold for $d \geq 3$ too.

Figure 1 (c) exemplifies a possible spin configuration and associated frozen and melting regions. One simple example of the frozen region is a ladder-like region along the lattice with all spins aligning up in the z direction, percolating the system from one end to the other (the area *A* in Fig. 1 (c)). Another example is a wider region in which not all the spins are aligned in the same direction (the region between the areas *B* and *C* in Fig. 1 (c)) and surrounds some melting regions. A spin configuration in a frozen region can also exhibit a checker-board pattern (the area *D* in Fig. 1 (c)). In all of the cases, every spin is arranged in such a way that at least $(d + 1)$ of its nearest-neighbor spins have the same direction, which set the value of $\hat{Q}_i$ to zero. Because this condition prohibits a frozen region to have corners under the periodic boundary conditions, we conjecture that all frozen regions percolate the system from one side to the other [70].

Because of the frozen regions, the Hilbert space has exponentially many subspaces. For example, a spin configuration having a frozen region cannot change into another spin configuration having a different frozen region by the Hamiltonian dynamics. This splits the Hilbert space into subspaces. Moreover, even when the arrangement of frozen regions is the same, there are many ways in which the DWs are spatially distributed over separated melting regions. Since the density of DW within each melting region is conserved over time, the Hilbert space is broken up into even smaller subspaces. Each subspace is therefore characterized by the configuration of the frozen regions and the spatial distribution of the DW density for melting regions.

The emergence of the dynamically fragmented subspaces suggests that the relaxation dynamics of the system strongly depends on the details of the initial state. When we take an

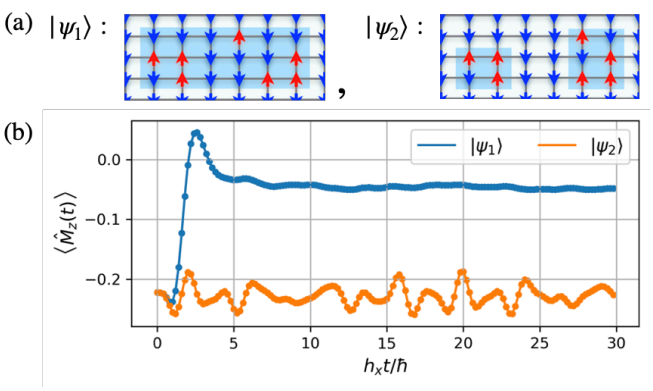

FIG. 2. (a) Spin configurations of the two initial states for $N = 3 \times 6$ lattice. We assume that the system is surrounded by fixed spins pointing down. Regions with blue shades show melting ones. (b) Magnetization dynamics starting from the two initial product states. Time evolution of the expectation value $\langle \hat{M}_z(t) \rangle := \langle \psi(t) | (1/N) \sum_i \hat{\sigma}_i^z | \psi(t) \rangle$ shows that a slightly different initial condition results in substantially different stationary states.

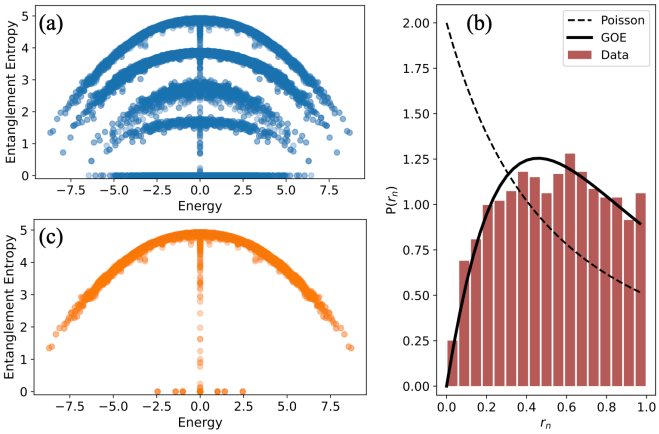

FIG. 3. (a) Entanglement entropy of all the energy eigenstates in a DW sector for a 3×6 lattice. At its boundaries, the system is surrounded by fixed frozen spins pointing down. In all panels (a)–(c), we take $n_{\rm DW} = 20$, for which $0 \le n_{\rm DW} \le 36$. We find that the entanglement entropy exhibits a broad distribution even for a fixed energy, indicating the breakdown of the ETH in this DW sector. (b) Distribution of the consecutive energy-gap ratio r_n [76] for the subspace without frozen regions. The statistics is calculated after resolving the two spatial inversion symmetries along the x and y directions [77]. Dashed line shows the Poisson prediction $P_{\rm Poisson}(r) = 2/(1+r)^2 \Theta(1-r)$ and the solid line shows the GOE prediction $P_{\rm GOE}(r) = (27/4)(r+r^2)/\left(1+r+r^2\right)^{5/2} \Theta(1-r)$, where Θ is the Heaviside step function. The agreement between the result and the GOE prediction indicates the non-integrability of the system defined in this subspace. (c) Entanglement entropy of the energy eigenstates in the subspace without frozen regions (extracted from the panel (a)). Most of the eigenstates with close energies have similar values of entanglement entropy, in accordance with the ETH. Meanwhile, a small number of low-entangled eigenstates appear around specific values: $E = 0, \pm 1, \pm\sqrt{2}$ and $\pm\sqrt{6}$, which are regarded as quantum many-body scars [55, 65–67, 70].

initial state from one of the subspaces in a given DW sector and let it evolve, the state remains in this subspace. Let us consider, for example, two initial product states $|\psi_1\rangle$ and $|\psi_2\rangle$ shown in Fig. 2 (a), which are slightly different in their spin configurations but have the same energy in a DW sector. Figure 2 (b) shows the dynamics of the expectation value of the magnetization density from these two initial product states according to the effective Hamiltonian $\hat{H}_{\rm eff}$. Throughout this paper, we perform numerical calculations under the condition that the spins constituting the system are surrounded by fixed frozen spins pointing down. Due to the frozen region in the middle of the lattice, which emerges only in the state $|\psi_2\rangle$, the magnetization relaxes to substantially different values for the two initial conditions, which indicates ergodicity breaking. This example highlights that a frozen region covering a large area of the system can be converted into a melting region with a small change in the initial configuration in this model. Similar behavior can be also observed under the time evolution by $\hat{H}$ with a weak h_x (see supplementary material [70]).

The non-ergodicity due to the HSF in this model is deeply related to the violation of the ETH. The fragmented structure yields exponentially many non-thermal energy eigenstates. Simple examples of such non-thermal states are product frozen states, which correspond to the states in isolated subspaces with the dimension one. As detailed in Supplemental Material [70], we show that the number of frozen states increases exponentially in the system size, indicating the emergence of the HSF [62]. We note that Ref. [9] also finds a similar frozen state for an effective model of TFIM on a pseudo-one-dimensional ladder, but no HSF was discussed there. As another example, we find eigenstates which have spatially inhomogeneous DW density owing to frozen regions that act as a wall to separate different melting regions.

Figure 3 (a) shows the entanglement entropy of all the energy eigenstates of $\hat{H}_1$ in a fixed DW sector for a 3 times 6 lattice [74]. We evaluate it by computing the von-Neumann entropy of the left half of the system. In generic systems obeying the ETH, eigenstate entanglement entropies are close to one another for close eigenenergies. In Fig. 3 (a), we demonstrate the violation of the ETH in this model, that is, a broad distribution of the entanglement entropy even for close eigenenergies and the presence of eigenstates with low entanglement. Due to the existence of frozen regions that divide the system into isolated parts, there are many eigenstates with zero bipartite entanglement [75].

Several remarks are in order. First, the kinetic constraint in $\hat{H}_1$ is associated with the conservation of the DW number alone. In particular, the model possesses frozen regions that dynamically divide the system and exhibits exponentially many frozen states. These properties are often found in the previously studied models [62] as a consequence of more than one conserved quantities [49–53, 57, 60]. Our finding here demonstrates that such nontrivial physics can occur even when there is only one apparent conserved quantity. Second, consequences of the percolation behavior of frozen regions

depend on d. For $d = 2$, the system is always divided into isolated parts by frozen regions that percolate the system and act as walls. However, for $d > 2$, frozen regions do not always divide the system because their shape can be, e.g., a square prism which percolates only in one direction along the lattice. It is also worth mentioning that the Hamiltonian Eq. 2 does not yield many frozen regions and the resultant HSF for $d = 1$, while we show in fact it does for $d > 1$. Finally, eigenstates with frozen regions can be found in every DW sector as long as the system is sufficiently large. Thus, non-ergodic behavior can be found for initial states with any finite energy density with respect to the effective Hamiltonian $\hat{H}_{\rm eff}$. This suggests that the original TFIM in a weak transverse field exhibits non-thermal behavior for long times at any energy scale for particular initial states.

Subspace properties. — Now we investigate properties of the fragmented subspaces of $\hat{H}_1$. Dynamics for each subspace is observed only in the melting regions, being characterized by their shapes and their boundary conditions. Here we specifically consider the case for $d = 2$ and show that there are a rich variety of dynamics in some melting regions, including those found in non-integrable, integrable, and quantum many-body scarred systems.

The Hamiltonian $\hat{H}_1$ itself is presumably non-integrable. To demonstrate this, let us choose a subspace having no frozen regions. In Fig. 3 (b), we perform the analysis of energy-level statistics for this subspace. We calculate the distribution of the consecutive energy-gap ratio $r_n = \min(\delta_n/\delta_{n-1}, \delta_{n-1}/\delta_n)$ with $\delta_n := E_{n+1} - E_n$, where E_n denotes the nth energy eigenvalue in the subspace [76]. The statistics of this ratio in Fig. 3 (b) shows a good agreement with that of the Gaussian Orthogonal Ensemble (GOE), indicating that this subspace as well as the entire $\hat{H}_1$ is non-integrable.

Additionally, in the subspace without frozen regions, we numerically find eigenstates with low entanglement in the bulk of the spectrum, which are regarded as quantum many-body scarred states [55, 65–67]. Figure 3 (c) demonstrates the presence of such states around $E = 0, \pm 1, \pm\sqrt{2}$ and $\pm\sqrt{6}$. The origin of these states cannot be attributed to frozen regions as they are excluded in this subspace. We find that some of them originate from specific local structures of the adjacency graph of the Hamiltonian [78, 79]; see supplementary material for details [70].

Interestingly, we find that the one-dimensional PXP model and the XX model can be embedded as melting regions of the model $\hat{H}_1$. First, let us discuss the emergent PXP model (see the area *B* in Fig. 1 (c)). In this one-dimensional region, all sites are adjacent to the frozen sites with up spins. Therefore, in this region, every spin can be flipped only when its two nearest neighbors are down due to the kinetic constraint. Hence, the system is effectively governed by

$$\hat{H}_B = \sum_{i \in B} \hat{\sigma}_i^x \frac{1}{4} \left(1 - \hat{\sigma}_{i+1}^z\right) \left(1 - \hat{\sigma}_{i-1}^z\right). \tag{4}$$

This is the one-dimensional PXP model, a well-known non-integrable model for hosting quantum many-body scars [66, 80–83]. This implies that one observes a long-lived oscillation of an observable in this one-dimensional region if we prepare an appropriate initial configuration. Second, let us briefly discuss the XX model (the area *C* in Fig. 1 (c)). In this region, the direction of the spin neighboring on the right side is opposite to that neighboring on the left side. We then find that the following Hamiltonian governs the dynamics in this region:

$$\hat{H}_C = \sum_{i \in C} \hat{\sigma}_i^x \frac{1}{2} \left(1 - \hat{\sigma}_{i+1}^z \hat{\sigma}_{i-1}^z\right). \tag{5}$$

This is the same as the effective Hamiltonian of the Ising chain in a weak transverse field [84] and is mappable to the XX chain [85], which is exactly solvable and thus ergodicity is broken due to the integrability. This implies that some subspaces become integrable when they only have a specific type of melting regions.

Conclusion and outlook. — In this Letter we have rigorously demonstrated that the effective model obtained from the d-dimensional Ising model in a weak transverse field on a hypercubic lattice exhibits the HSF for $d \geq 2$. In particular, the kinetic constraint, which is attributed to the emergent conservation of the DW number in this model, forms frozen regions that percolate the system. Consequently, each DW sector fractures into exponentially many isolated subspaces, leading to the violation of the ETH. We furthermore showed that some of the subspaces can be non-integrable, integrable, and even possess scarred eigenstates. Our results indicate that nontrivial initial-state dependence is observed for prethermal dynamics of the Ising models in a weak transverse field. Because the TFIM in two and three dimensions are experimentally realizable [5, 86–92], we believe that the model serves as a novel platform for observing the signatures of HSF, which is distinct from previous experiments that required, e.g., tilted potentials [93, 94]. We leave it for future work to investigate the robustness of transient non-ergodicity under long-range Ising interaction, which often arises in experiments. Finally, given that $\hat{H}_{\rm eff}$ is obtained in the weak-field limit of the TFIM, it is interesting to see how properties of the Ising model without the transverse field, such as (classical) integrability and finite-temperature phase transition, affect physics in our model.

Acknowledgments. — We are grateful to Naomichi Hatano for fruitful discussion and carefully reading the manuscript, and Rahul Nandkishore for insightful comments. AY thanks Junichi Haruna for useful discussion. This work was supported by Leading Initiative for Excellent Young Researchers MEXT Japan, JST PRESTO (Grant No. JPMJPR1919) Japan, JST COI-NEXT program (JPMJPF2014), and MEXT Quantum Leap Flagship Program (MEXT Q-LEAP) Grant Number JPMXS0120319794.

* yoshi9d@iis.u-tokyo.ac.jp
† matsuzaki.yuichiro@aist.go.jp
‡ ryusuke.hamazaki@riken.jp

[1] P. De Gennes, Solid State Communications **1**, 132 (1963).
[2] R. Stinchcombe, Journal of Physics C: Solid State Physics **6**, 2459 (1973).
[3] K. R. Fratus and M. Srednicki, Physical Review E **92**, 040103 (2015).
[4] R. Mondaini, K. R. Fratus, M. Srednicki, and M. Rigol, Physical Review E **93**, 032104 (2016).
[5] E. Guardado-Sanchez, P. T. Brown, D. Mitra, T. Devakul, D. A. Huse, P. Schauß, and W. S. Bakr, Physical Review X **8**, 021069 (2018).
[6] M. Schmitt and M. Heyl, Physical Review Letters **125**, 100503 (2020).
[7] J. Richter, T. Heitmann, and R. Steinigeweg, SciPost Physics **9**, 031 (2020).
[8] B. Blaß and H. Rieger, Scientific reports **6**, 1 (2016).
[9] B. van Voorden, J. Minář, and K. Schoutens, Physical Review B **101**, 220305 (2020).
[10] J. M. Deutsch, Physical review a **43**, 2046 (1991).
[11] M. Srednicki, Physical review e **50**, 888 (1994).
[12] H. Tasaki, Physical review letters **80**, 1373 (1998).
[13] S. Goldstein, J. L. Lebowitz, R. Tumulka, and N. Zanghì, Physical review letters **96**, 050403 (2006).
[14] S. Popescu, A. J. Short, and A. Winter, Nature Physics **2**, 754 (2006).
[15] M. Rigol, V. Dunjko, and M. Olshanii, Nature **452**, 854 (2008).
[16] P. Reimann, Physical review letters **101**, 190403 (2008).
[17] S. Goldstein, J. L. Lebowitz, C. Mastrodonato, R. Tumulka, and N. Zanghi, Physical Review E **81**, 011109 (2010).
[18] M. Rigol and M. Srednicki, Physical review letters **108**, 110601 (2012).
[19] C. Gogolin and J. Eisert, Reports on Progress in Physics **79**, 056001 (2016).
[20] H. Tasaki, Journal of Statistical Physics **163**, 937 (2016).
[21] F. H. Essler and M. Fagotti, Journal of Statistical Mechanics: Theory and Experiment **2016**, 064002 (2016).
[22] P. Reimann, Journal of Statistical Mechanics: Theory and Experiment **2021**, 103106 (2021).
[23] T. Kinoshita, T. Wenger, and D. S. Weiss, Nature **440**, 900 (2006).
[24] A. Polkovnikov, K. Sengupta, A. Silva, and M. Vengalattore, Reviews of Modern Physics **83**, 863 (2011).
[25] M. Gring, M. Kuhnert, T. Langen, T. Kitagawa, B. Rauer, M. Schreitl, I. Mazets, D. A. Smith, E. Demler, and J. Schmiedmayer, Science **337**, 1318 (2012).
[26] M. Schreiber, S. S. Hodgman, P. Bordia, H. P. Lüschen, M. H. Fischer, R. Vosk, E. Altman, U. Schneider, and I. Bloch, Science **349**, 842 (2015).
[27] A. M. Kaufman, M. E. Tai, A. Lukin, M. Rispoli, R. Schittko, P. M. Preiss, and M. Greiner, Science **353**, 794 (2016).
[28] J. Smith, A. Lee, P. Richerme, B. Neyenhuis, P. W. Hess, P. Hauke, M. Heyl, D. A. Huse, and C. Monroe, Nature Physics **12**, 907 (2016).
[29] H. Labuhn, D. Barredo, S. Ravets, S. De Léséleuc, T. Macrì, T. Lahaye, and A. Browaeys, Nature **534**, 667 (2016).
[30] G. Kucsko, S. Choi, J. Choi, P. C. Maurer, H. Zhou, R. Landig, H. Sumiya, S. Onoda, J. Isoya, F. Jelezko, E. Demler, N. Y. Yao, and M. D. Lukin, Physical review letters **121**, 023601 (2018).
[31] R. V. Jensen and R. Shankar, Physical review letters **54**, 1879 (1985).
[32] H. Kim, T. N. Ikeda, and D. A. Huse, Physical Review E **90**, 052105 (2014).
[33] A. Khodja, R. Steinigeweg, and J. Gemmer, Physical Review E **91**, 012120 (2015).
[34] L. D'Alessio, Y. Kafri, A. Polkovnikov, and M. Rigol, Advances in Physics **65**, 239 (2016).
[35] J. R. Garrison and T. Grover, Physical Review X **8**, 021026 (2018).
[36] T. Yoshizawa, E. Iyoda, and T. Sagawa, Physical review letters **120**, 200604 (2018).
[37] S. Sugimoto, R. Hamazaki, and M. Ueda, Physical Review Letters **126**, 120602 (2021).
[38] S. Sugimoto, R. Hamazaki, and M. Ueda, arXiv preprint arXiv:2111.12484 (2021).
[39] M. Rigol, V. Dunjko, V. Yurovsky, and M. Olshanii, Physical review letters **98**, 050405 (2007).
[40] R. Steinigeweg, J. Herbrych, and P. Prelovšek, Physical Review E **87**, 012118 (2013).
[41] P. Calabrese, F. H. Essler, and G. Mussardo, Journal of Statistical Mechanics: Theory and Experiment **2016**, 064001 (2016).
[42] L. Vidmar and M. Rigol, Journal of Statistical Mechanics: Theory and Experiment **2016**, 064007 (2016).
[43] A. Pal and D. A. Huse, Physical review b **82**, 174411 (2010).
[44] R. Nandkishore and D. A. Huse, Annu. Rev. Condens. Matter Phys. **6**, 15 (2015).
[45] M. Serbyn, Z. Papić, and D. A. Abanin, Physical review letters **111**, 127201 (2013).
[46] D. A. Huse, R. Nandkishore, and V. Oganesyan, Physical Review B **90**, 174202 (2014).
[47] D. A. Abanin, E. Altman, I. Bloch, and M. Serbyn, Reviews of Modern Physics **91**, 021001 (2019).
[48] G. De Tomasi, D. Hetterich, P. Sala, and F. Pollmann, Physical Review B **100**, 214313 (2019).
[49] S. Moudgalya, A. Prem, R. Nandkishore, N. Regnault, and B. A. Bernevig, arXiv preprint arXiv:1910.14048 (2019).
[50] P. Sala, T. Rakovszky, R. Verresen, M. Knap, and F. Pollmann, Physical Review X **10**, 011047 (2020).
[51] V. Khemani, M. Hermele, and R. Nandkishore, Physical Review B **101**, 174204 (2020).
[52] Z.-C. Yang, F. Liu, A. V. Gorshkov, and T. Iadecola, Physical review letters **124**, 207602 (2020).
[53] T. Rakovszky, P. Sala, R. Verresen, M. Knap, and F. Pollmann, Physical Review B **101**, 125126 (2020).
[54] H. Zhao, J. Vovrosh, F. Mintert, and J. Knolle, Physical review letters **124**, 160604 (2020).
[55] M. Serbyn, D. A. Abanin, and Z. Papić, Nature Physics **17**, 675 (2021).
[56] K. Lee, A. Pal, and H. J. Changlani, Physical Review B **103**, 235133 (2021).
[57] A. Khudorozhkov, A. Tiwari, C. Chamon, and T. Neupert, arXiv preprint arXiv:2107.09690 (2021).
[58] B. Mukherjee, D. Banerjee, K. Sengupta, and A. Sen, Physical Review B **104**, 155117 (2021).
[59] B. Buča, Phys. Rev. Lett. **128**, 100601 (2022).
[60] A. Bastianello, U. Borla, and S. Moroz, Phys. Rev. Lett. **128**, 196601 (2022).
[61] S. Moudgalya and O. I. Motrunich, Phys. Rev. X **12**, 011050 (2022).
[62] S. Moudgalya, B. A. Bernevig, and N. Regnault, Reports on Progress in Physics **85**, 086501 (2022).
[63] R. M. Nandkishore and M. Hermele, Annual Review of Condensed Matter Physics **10**, 295 (2019).
[64] M. Pretko, X. Chen, and Y. You, International Journal of Modern Physics A **35**, 2030003 (2020).
[65] S. Moudgalya, N. Regnault, and B. A. Bernevig, Physical Review B **98**, 235156 (2018).
[66] C. J. Turner, A. A. Michailidis, D. A. Abanin, M. Serbyn, and Z. Papić, Nature Physics **14**, 745 (2018).

[67] Z. Papić, arXiv preprint arXiv:2108.03460 (2021).

[68] D. Abanin, W. De Roeck, W. W. Ho, and F. Huveneers, Communications in Mathematical Physics **354**, 809 (2017).

[69] T. Close, F. Fadugba, S. C. Benjamin, J. Fitzsimons, and B. W. Lovett, Physical review letters **106**, 167204 (2011).

[70] See Supplemental Material, which includes Refs. [95–100], for (i) the expression of $\hat{Q}_i$ in arbitrary dimensions, (ii) numerical estimation of the timescale over which our effective model works well, (iii) a reason for the conjecture that frozen regions should percolate the system, (iv) analytic demonstration of the exponentially growing number of the subspaces, and (v) numerical and some exact results on the special eigenstates which are found in Fig. 3 (c).

[71] Z. Gong, N. Yoshioka, N. Shibata, and R. Hamazaki, Physical Review A **101**, 052122 (2020).

[72] Z. Gong, N. Yoshioka, N. Shibata, and R. Hamazaki, Physical Review Letters **124**, 210606 (2020).

[73] The DW number conservation law and the chiral symmetry appear both in a periodic boundary condition and an open boundary condition.

[74] When numerically diagonalizing the Hamiltonian for (a) and (c), we added perturbative random longitudinal fields with average strength 10^{-5}. This is due to avoid ambiguity caused by exact degeneracy originating from unwanted symmetries such as inversion.

[75] The distribution at $E = 0$ in Fig. 3 (a) and (b) still involves some ambiguity because of degeneracy of an exponentially large number of zero-energy states. This may imply that the degeneracy originates from not only the chiral symmetry and spatial inversion symmetry [101] but also some hidden ones, which are not broken by the additional longitudinal fields.

[76] Y. Y. Atas, E. Bogomolny, O. Giraud, and G. Roux, Physical review letters **110**, 084101 (2013).

[77] Note that the GOE distribution is obtained only after resolving apparent symmetries, whereas the Poisson-like distribution often appears when symmetries such as inversion are unresolved [4, 34, 102, 103].

[78] J.-Y. Desaules, A. Hudomal, C. J. Turner, and Z. Papić, Physical Review Letters **126**, 210601 (2021).

[79] F. M. Surace, M. Dalmonte, and A. Silva, arXiv preprint arXiv:2107.00884 (2021).

[80] H. Bernien, S. Schwartz, A. Keesling, H. Levine, A. Omran, H. Pichler, S. Choi, A. S. Zibrov, M. Endres, M. Greiner, V. Vuleti, and M. D. Lukin, Nature **551**, 579 (2017).

[81] C. J. Turner, A. A. Michailidis, D. A. Abanin, M. Serbyn, and Z. Papić, Physical Review B **98**, 155134 (2018).

[82] C.-J. Lin and O. I. Motrunich, Physical review letters **122**, 173401 (2019).

[83] T. Iadecola, M. Schecter, and S. Xu, Physical Review B **100**, 184312 (2019).

[84] J.-S. Lee and A. K. Khitrin, Physical Review A **71**, 062338 (2005).

[85] M. Ostmann, M. Marcuzzi, J. P. Garrahan, and I. Lesanovsky, Physical Review A **99**, 060101 (2019).

[86] M. W. Johnson, M. H. S. Amin, S. Gildert, T. Lanting, F. Hamze, N. Dickson, R. Harris, A. J. Berkley, J. Johansson, P. Bunyk, E. M. Chapple, C. Enderud, J. P. Hilton, K. Karimi, E. Ladizinsky, N. Ladizinsky, T. Oh, I. Perminov, C. Rich, M. C. Thom, E. Tolkacheva, C. J. S. Truncik, S. Uchaikin, J. Wang, B. Wilson, and G. Rose, Nature **473**, 194 (2011).

[87] J. G. Bohnet, B. C. Sawyer, J. W. Britton, M. L. Wall, A. M. Rey, M. Foss-Feig, and J. J. Bollinger, Science **352**, 1297 (2016).

[88] A. Kumar, T.-Y. Wu, F. Giraldo, and D. S. Weiss, Nature **561**, 83 (2018).

[89] A. Browaeys and T. Lahaye, Nature Physics **16**, 132 (2020).

[90] Y. Song, M. Kim, H. Hwang, W. Lee, and J. Ahn, Physical Review Research **3**, 013286 (2021).

[91] S. Ebadi, T. T. Wang, H. Levine, A. Keesling, G. Semeghini, A. Omran, D. Bluvstein, R. Samajdar, H. Pichler, W. W. Ho, S. Choi, S. Sachdev, M. Greiner, V. Vuleti, and M. D. Lukin, Nature **595**, 227 (2021).

[92] P. Scholl, M. Schuler, H. J. Williams, A. A. Eberharter, D. Barredo, K.-N. Schymik, V. Lienhard, L.-P. Henry, T. C. Lang, T. Lahaye, A. M. Luchli, and A. Browaeys, Nature **595**, 233 (2021).

[93] S. Scherg, T. Kohlert, P. Sala, F. Pollmann, B. H. Madhusudhana, I. Bloch, and M. Aidelsburger, Nature Communications **12**, 1 (2021).

[94] T. Kohlert, S. Scherg, P. Sala, F. Pollmann, B. H. Madhusudhana, I. Bloch, and M. Aidelsburger, arXiv preprint arXiv:2106.15586 (2021).

[95] S. Kirkpatrick and T. P. Eggarter, Physical Review B **6**, 3598 (1972).

[96] B. Sutherland, Physical Review B **34**, 5208 (1986).

[97] R. Bueno and N. Hatano, Physical Review Research **2**, 033185 (2020).

[98] C.-J. Lin, V. Calvera, and T. H. Hsieh, Physical Review B **101**, 220304 (2020).

[99] H. Zhao, A. Smith, F. Mintert, and J. Knolle, Physical Review Letters **127**, 150601 (2021).

[100] O. Hart and R. Nandkishore, arXiv preprint arXiv:2203.06188 (2022).

[101] M. Schecter and T. Iadecola, Physical Review B **98**, 035139 (2018).

[102] A. Gubin and L. F. Santos, American Journal of Physics **80**, 246 (2012).

[103] R. Hamazaki, T. N. Ikeda, and M. Ueda, Physical Review E **93**, 032116 (2016).